Incoherent Inelastic Neutron Scattering Studies of Nanoconfined Water in Clinoptilolite and Heulandite Zeolites

ARTICLE *in* THE JOURNAL OF PHYSICAL CHEMISTRY C · AUGUST 2008

Impact Factor: 4.77 · DOI: 10.1021/jp803770v

5 AUTHORS, INCLUDING:

Monika Hartl
European Spallation Source (ESS)
78 PUBLICATIONS **370** CITATIONS

SEE PROFILE

Incoherent Inelastic Neutron Scattering Studies of Nanoconfined Water in Clinoptilolite and Heulandite Zeolites

Nathan W. Ockwig,[†] Randall T. Cygan,[†] Monika A. Hartl,[§] Luke L. Daemen,[§] and Tina M. Nenoff*,[‡]

Geochemistry Department and Surface and Interface Sciences Department, Sandia National Laboratories, P. O. Box 5800, Albuquerque, New Mexico 87185, and Manuel Lujan, Jr. Neutron Scattering Center LANSCE-LC, Los Alamos National Laboratory, P. O. Box 1663, Los Alamos, New Mexico 87545

Received: April 29, 2008; Revised Manuscript Received: June 23, 2008

In a continued effort studying the role of water in ion exchange processes of zeolites, a synthetic series of alkali and alkaline earth metal cation variants (Na^+, K^+, Rb^+, Mg^{2+}, and Ca^{2+}) of the hydrated clinoptilolite (Si/Al $\approx$ 5) and heulandite (Si/Al $\approx$ 3.5) aluminosilicate zeolites is examined by incoherent inelastic neutron scattering (IINS). The low-frequency librational modes of water reveal the impact of nanoconfinement and framework charge within these isostructural aluminosilicate structures. The experimental IINS spectra are correlated with power spectra derived through molecular dynamics simulations. The impact of ion−zeolite, ion−water, and water−zeolite interactions on the hindered rotations (librations) of water molecules is explored as a function of Si/Al substitution, cation identity, and subnanometer confinement. The results indicate that electrostatic charge on the overall framework has a stronger influence than charge density of a given ion in the channel and that these effects become more pronounced as the charge difference between ion and zeolite is increased.

Introduction

Currently, the structural and dynamic behavior of bulk water is relatively well understood and documented.[1−8] However, there are comparatively few efforts focused on the behavior of water under angstrom-level confinement. The study of nanoconfined molecular species is a surprisingly difficult topic which relies on a variety of experimental methods and continues to challenge our theoretical understanding.[9−16] Nanoconfined water is arguably the most important molecular species in porous materials because of its tremendous impact across many industrially significant and interdisciplinary processes.[12] It is reasonable to assume that the properties of confined and bulk water are similar. However, there are a growing number of reports which clearly indicate that such assumptions should be reconsidered.[17] The molecular structure of water is deceptively simple while the collective behavior of these species is quite complex, especially under nanoconfinement. It remains a major challenge for current scientific understanding and levels of theory.[18] Quantification of confined molecular behavior is the foundation necessary to understand macroscopic phenomena and ultimately provides the basis for understanding, modifying, and directing important macroscopic observables and physical properties. There are many porous systems of interest including zeolites, which are perhaps the most well studied within the context of confined water.[19−26]

Dynamic Behavior of Water

The multiple intramolecular vibrational and librational/rotational modes of water give it distinct spectroscopic signatures. The *intramolecular* bending and stretching modes commonly occur at ~1600 and 3300−3700 cm^{-1}, respectively, and the *intermolecular* librational/rotational modes occur from 300 to 1100 cm^{-1}. The low-frequency (librational) modes are extremely sensitive to localized hydrogen bonding and steric restrictions from nanoscale confinement and consequently have more pronounced spectroscopic shifts. Thus, librational/rotational spectroscopy is a vital diagnostic tool for examining water behavior within porous media.

Additionally, the structural and dynamic properties of water in different localized environments have been probed using a wide variety of theoretical and experimental approaches.[22,25−30] Among the most commonly employed methods to probe the intra- and intermolecular behavior of water are Raman scattering,[31] microwave and infrared spectroscopies,[32] nuclear magnetic resonance (NMR),[33,39] molecular dynamics (MD),[34−39] X-ray diffraction,[40] neutron diffraction,[41] and incoherent quasi-elastic and incoherent inelastic neutron scattering (IQENS and IINS, respectively).[12,39,42−45] There is an impressive body of literature on the role of water in thermodynamic, dynamic, and structural processes and the properties which have been probed through a variety of, often complementary, methods. Although these methods and studies provide internally consistent results, there are many conflicting studies and conclusions which are fueling the continuous revision of our theoretical understanding surrounding the behavior of nanoconfined water.

The complex interactions and equilibria which exist among four distinct interactions control the dynamic behavior of nanoconfined water in materials such as zeolites. In no particular order, these are (1) H_2O-H_2O, (2) ion−H_2O, (3) H_2O−framework, and (4) ion−framework. Although ion−ion electrostatic repulsions may have an impact by separation of localized water attractors, this effect is essentially negligible due to charge screening of the surrounding zeolite framework. Other studies on occluded water have presented evidence for

* To whom correspondence should be addressed. Telephone: (505) 844-0340. Fax: (505) 844-5470. E-mail: tmnenof@sandia.gov.
† Geochemistry Department, Sandia National Laboratories.
‡ Surface and Interface Sciences Department, Sandia National Laboratories.
§ Los Alamos National Laboratory.

10.1021/jp803770v CCC: $40.75
Published on Web 08/12/2008

TABLE 1: Synthetic Parameters for the Preparation of Alkali and Alkali Earth Metal Members of the Clinoptilolite (CLI_{mono} and CLI_{di}, Respectively) and Heulandite (HEU_{mono} and HEU_{di}, Respectively) Series

sample	reactant composition	temp (°C)	time (h)	pH[b]	Si/Al[c]
Na−CLI	15 NaOH/9 $Al(OH)_3$/50 SiO_2/521 H_2O	145	156	11.6	5.0
K−CLI	15 KOH/9 $Al(OH)_3$/50 SiO_2/537 H_2O	185	96	10.1	5.1
Rb−CLI	15 RbOH/9 $Al(OH)_3$/50 SiO_2/593 H_2O	185	120	10.7	5.4
Mg−CLI	14 $MgCO_3$/9 $Al(OH)_3$/50 SiO_2/604 H_2O	205	178	9.9	4.8
Ca−CLI	14 $CaCO_3$/9 $Al(OH)_3$/50 SiO_2/616 H_2O	205	180	9.8	4.7
Na−HEU[a]	18 NaOH/10 $Al(OH)_3$/38 SiO_2/616 H_2O	135	132	11.4	3.7
K−HEU[a]	18 KOH/10 $Al(OH)_3$/38 SiO_2/616 H_2O	185	90	9.6	3.5
Rb−HEU[a]	18 RbOH/10 $Al(OH)_3$/38 SiO_2/616 H_2O	185	108	10.1	3.4
Mg−HEU[a]	16 $MgCO_3$/10 $Al(OH)_3$/45 SiO_2/616H_2O	200	172	9.7	3.1
Ca−HEU[a]	16 $CaCO_3$/10 $Al(OH)_3$/45 SiO_2/616 H_2O	200	178	9.8	3.3

[a] Required addition of 5% (w/w) seed crystals of natural heulandite, from the Nasik deposit near Maharashtra, India. [b] pH of postsynthesis mother liquor. [c] Measured by SEM−EDS, ±5%.

the presence of ice-like water in small-pore zeolitic systems with highly constrained waters exhibiting ion−H_2O and H_2O−framework interactions.[9−11,39] Furthermore, hydration and dehydration processes, cation mobility, and framework stability have been studied in mesoporous systems.[46] Our present study focuses on the librational (hindered rotational motion) behavior of water rather than hydration and dehydration processes, cation mobility, or framework stability which have been previously investigated for a variety of mesoporous materials by several other research teams.[47]

In this contribution, we probe changes in the librational behavior of confined water molecules in a series of synthetic large-pore heulandite and clinoptilolite zeolites through low temperature IINS studies. This is an experimental extension to complement and validate our previous MD simulations.[9,12] The two zeolites were specifically targeted to avoid the challenging topic of zeolite structural variations and their impact on occluded H_2O interactions. However, studying these two closely related zeolites allows us to address several fundamental questions relating to the role of framework charge and cation type on confined water dynamics.

Experimental Procedure

Chemical sources were aluminum hydroxide (USP) from Pfaltz and Bauer, Inc., Ludox LS colloidal silica 30% (w/w) silica, sodium hydroxide, potassium hydroxide, rubidium hydroxide (50% aqueous solution), magnesium carbonate, and calcium carbonate from Aldrich Chemical Corporation.

Synthetic preparations of the zeolite phases were adapted from those reported by Zhao, Szostak, and Kevan.[48] Crystallizations were carried out in Teflon-lined stainless steel autoclaves under autogenous pressure from a gel. A typical synthesis yields 8.27 g of good quality crystal crystalline powder. Dried aluminum hydroxide ($Al(OH)_3$, 0.78 g) was added to 6 M aqueous solution of sodium hydroxide (3.41 g). The mixture was vigorously stirred for 1 h, after which colloidal silica (Ludox LS, 10 g) was added. The mixture was stirred for an additional 1 h and then placed into a Teflon-lined steel autoclave. The autoclave was heated to 145 °C at a rate of 2 °C/min and held for 156 h. Reactant molar compositions, reaction conditions, final pH values of the postsynthesis mother liquid, and resulting Si/Al ratios are summarized in Table 1. Sample hydration was performed by placing fully dehydrated samples in a hydration chamber (85 °C, 100% relative humidity) for 6 h. Thermal gravimetric analysis (TGA) of all samples revealed ~22 water molecules (~90% hydrated) per idealized formula unit (heulandite, $X_8Si_{28}Al_8O_{72}\cdot 24H_2O$; clinoptilolite, $X_6Si_{30}Al_6O_{72}\cdot 24H_2O$).[49] The potassium endmember of clinoptilolite was produced following the same procedure, however using potassium hydroxide rather than sodium hydroxide. The rubidium analogue of clinoptilolite was synthesized through the use of commercially available 50% w/w aqueous rubidium hydroxide−rubidium solution. Our initial attempts to synthesize heulandite were quite unsuccessful until 5% w/w of a natural sample (calcium heulandite from the Nasik deposit near Maharashtra, India) was added to the reactions as a nucleating seed material. Phase purity was confirmed by X-ray powder diffraction (XRPD), while Si/Al ratios and composition were determined by scanning electron microscopy−energy dispersive spectroscopy (SEM−EDS) and elemental analysis (EA).[50−52]

Heulandite and clinoptilolite are isostructural porous crystalline frameworks (both with the HEU framework type) with varying Si/Al ratios ranging from 2.5 to 6. Those with Si/Al ratios <4 are defined as heulandite (HEU), while those with ratios >4 are referred to as clinoptilolite (CLI). The framework is composed of three distinct types of channels—one defined by 10T rings and two others by 8T rings—which are interconnected to form a layered array of channels. One of the 8T channels (3.6 × 4.6 Å) and the 10T channel (3.1 × 7.5 Å) run parallel to the *c*-axis. Additionally, an interconnected plane of channels is formed by the remaining 8T channel (2.8 × 4.7 Å) which runs parallel to the *a*-axis and intersects the first two channels. Both materials crystallize in the monoclinic space group *C*2/*m* with slightly different unit cell parameters.[53]

Incoherent Inelastic Neutron Scattering (IINS). The Filter Difference Spectrometer (FDS) of the Los Alamos Neutron Science Center (LANSCE) is used for vibrational and rotational spectroscopies by incoherent inelastic neutron scattering. The instrument is designed for high count rates using a large 3 sr (9848.4 deg^2) solid-angle detector.

Neutrons are a unique probe for the study of molecular dynamics in hydrogen-containing solids and liquids. In particular, incoherent inelastic neutron scattering is ideally suited for molecular rotational modes because of its sensitivity to *intermolecular* motions relative to the higher frequency *intramolecular* vibrations. Of particular interest for this study are the low-frequency librational modes of water molecules which arise from hindered rotations within a given channel. While Si, Al, and O have very low incoherent scattering cross sections, ^1H has a very large incoherent neutron scattering cross section (80 barns). On this basis IINS represents the ideal probe for examining the behavior of nanoconfined water in microporous aluminosilicate zeolites. In fact, the *IINS spectrum is completely dominated by the scattering contributions from hydrogen* with

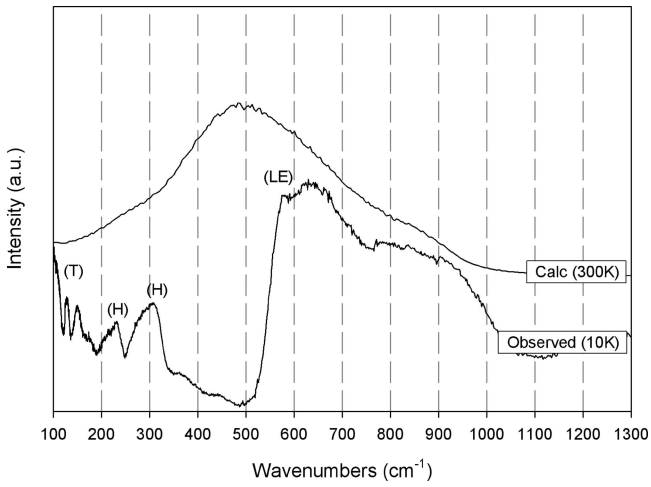

Figure 1. (upper) Low-frequency regions of the power spectrum of liquid water at 300 K derived from MD simulations. (lower) Observed IINS spectrum for ice Ih at 10 K. LE, librational edge; H, hydrogen-bond bending and stretching; T, translational modes.[58] (1 $cm^{-1} = 0.1240$ meV). Reproduced by permission of the PCCP Owner Societies, http://dx.doi.org/10.1039/b711949f.[12]

minimal contribution from other species. In addition, nucleus−neutron interactions do not have any of the photon−electron selection rules and therefore all modes are readily observed.

The IINS spectrum of each hydrated zeolite sample was measured to specifically examine the *inter*molecular interactions of water as manifested by changes in the librational (rotational) spectrum which usually occur from 300 to 1100 cm^{-1}. The librational spectrum arises from molecular motions which have a nonzero angular moment component. This produces three distinctly different rotational modes for molecular water (rocking, twisting, and wagging) ranging from 500 to 1000 cm^{-1} which are typically broad and often merge into a single broad feature, rendering the discrete rotational modes indistinguishable from one another. The librational modes are highly dependent on the local environment, position, and ordering of water. Sharp librational features are typically observed in cases where water is highly ordered in a crystalline lattice, while broadening of the librational signals is a direct consequence of disordered "bulk-like" water where multiple energetically close configurations coexist and produce a continuum of librational features. Broadening also arises from the Debye−Waller[54] factor; however, this is relatively small compared to the intrinsic width of the librational modes.

The confluence of libration modes produces a single extremely broad (~500 cm^{-1}) feature rendering many data sets very difficult to interpret; however, for these data deconvolution with a single coalescence was rigorously fit.[55] In cases where water is heavily restricted or isolated (through hydrogen bonding or related steric effects), these modes can become noticeably sharp, pronounced, and readily observable in IINS experiments.[56,57] Therefore, changes in local environment can have dramatic effects on peak positions, widths, and intensities. Generally, though, frequency increases and peak width decreases as rotational restrictions are increased through hydrogen bonding or steric effects. Despite significant experimental and theoretical efforts, the absolute assignment of discrete wagging, twisting, and rocking modes remains problematic. Often the onset of the librational features, referred to as the librational edge, is the only definitive spectroscopic assignment which is quantified in IINS experiments of ice Ih (Figure 1). However, even merged, the intensities of the soft librational features are significant and can be quantitatively predicted because of the simplicity of neutron−nucleus interactions.[57]

Results and Discussion

The librational spectra of each ion−zeolite pair (Na^+, K^+, Rb^+, Mg^{2+}, Ca^{2+} of CLI and HEU) were measured at 10 K (Figure 2). The libration IINS spectra for the clinoptilolite series (Figure 2A and 2B, CLI_{mono} and CLI_{di}, respectively) are compared, and then the heulandite series (Figure 2C and 2D, HEU_{mono} and HEU_{di}, respectively) follow by a cross comparison of (1) monovalent series versus the divalent series and (2) between the observed IINS data and simulated power spectra[12] for each zeolite−ion pair.

Each IINS spectrum in the CLI_{mono} series shows a single broad librational feature with no uniquely distinguishable wagging, rocking, or twisting modes. The data show a rough linear trend in librational shift ranging from 591 cm^{-1} for Na^+ to 637 cm^{-1} for Rb^+. This trend corresponds to a shift to higher frequency as the extraframework cation charge density decreases. The IINS spectra of the CLI_{di} series also exhibit a single broad librational feature with no uniquely distinguishable wagging, rocking, or twisting modes. The data show a trend in librational shift ranging from 651 cm^{-1} for Mg^{2+} to 633 cm^{-1} for Ca^{2+}, illustrating a correlation of shifts to higher frequency with increasing extraframework cation charge density.

The IINS spectra for the HEU_{mono} series also show a single broad librational feature with no uniquely identifiable wagging, rocking, or twisting modes. The observed trend (similar to that of CLI_{mono}) in the HEU_{mono} librational data shifts to higher frequency as charge density decreases on the extraframework cations. Both IINS spectra in the HEU_{di} series show single broad librational features with no discrete wagging, rocking, or twisting modes as observed for other systems. In the HEU_{di} series the observed libration peak shifts to higher frequency as the charge density of the extraframework cation increases, similar to the trend observed for the CLI_{di} series.

Comparison of the IINS data for the monovalent series (both CLI and HEU) shows nearly equivalent librational spectra (on a per ion basis) and virtually identical trends in librational shifts where frequency increases as a function of decreasing ion charge density ($Na^+ < K^+ < Rb^+$) for either zeolite. The IINS data for the divalent endmembers (both CLI and HEU) also show a significant degree of similarity in overall trend; however, the HEU_{di} data are shifted to higher overall librational frequency.

Comparison of the divalent endmembers (Figure 2C,D) reveals a significant difference between the trends in power spectra and observed librational spectra for CLI_{di} versus HEU_{di}. In the power spectra of the CLI_{di} system, increasing ion charge density ($Ba^{2+} < Sr^{2+} < Ca^{2+} < Mg^{2+}$) results in a shift of the librational maxima to higher frequency ($Ba^{2+} < Sr^{2+} < Ca^{2+} < Mg^{2+}$); the opposite is observed in the HEU_{di} series. The observed correlation of charge density with librational frequency is made possible because molecular dynamics simulations explicitly model atomic charge density through the force field parameters which are validated by empirical data from a variety of oxide, mineral, and zeolite phases.

Correlation and Comparison of IINS with MD Power Spectra. We further examined the trends in the IINS spectra by placing them within the context of our recent MD simulations[12] of nanoconfined water in aluminosilicate zeolites (Figure 3) and the derived power spectra. Although the entire series of cation-substituted zeolites was not experimentally measured—not all cation endmember compositions can be synthesized—the correspondence of experimental and theoretical data strongly

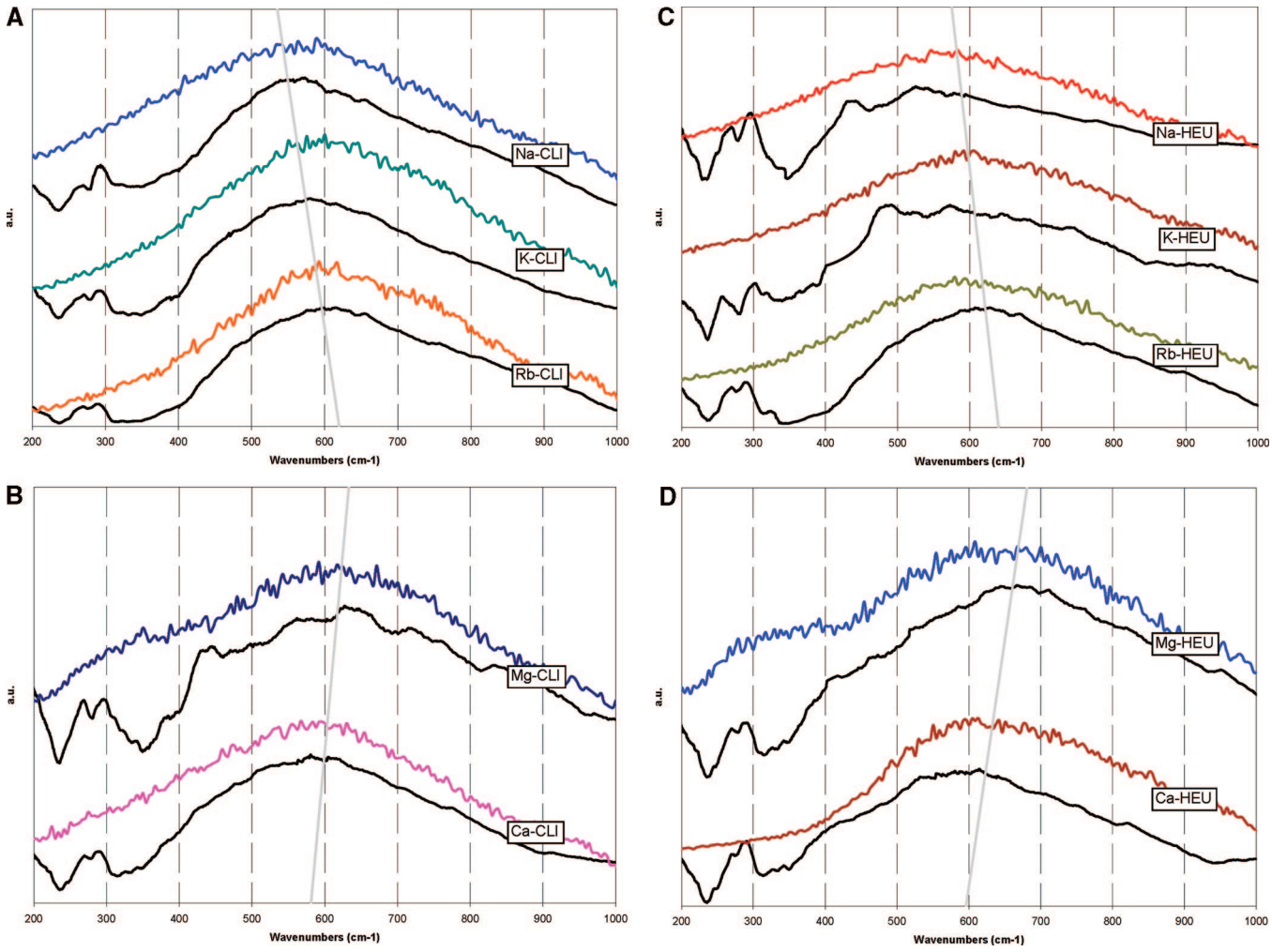

Figure 2. Simulated and measured librational region of IINS spectra at 10 K confined in (A) clinoptilolite with alkali metal ions (CLI_{mono}), (B) clinoptilolite with alkaline earth metal ions (CLI_{di}), (C) heulandite with alkali metal ions (HEU_{mono}), and (D) heulandite with alkaline earth metal ions (HEU_{di}). In each data set, the simulated data is the lower black line, and the experimental data is the upper colored line. The simulated data are derived from molecular dynamics trajectories at 300 K. Gray line represents the general trend in each respective data set (values determined through single peak deconvolution[54]).

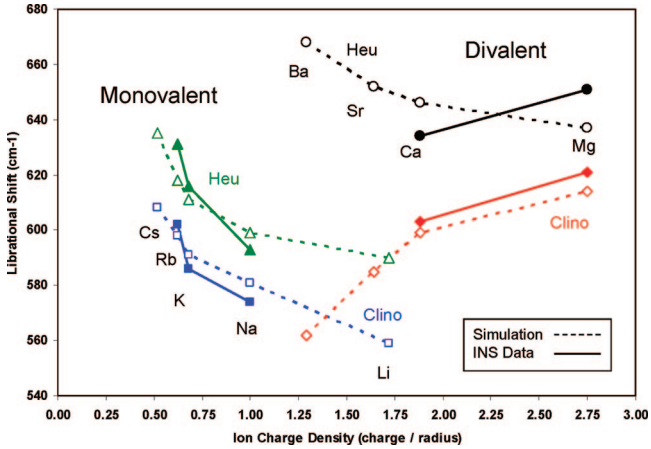

Figure 3. Librational shifts (cm^{-1}) of the monovalent alkali metal and divalent alkaline earth metal series versus ion charge density. Theoretical values of clinoptilolite (CLI) and heulandite (HEU) librational shifts are represented by dashed lines,[12] while the shifts observed by IINS are represented by solid lines.

suggests that trends can be established for librational interpretations and that they are indeed affected by the balance among the strength of zeolite, ion, and water interactions. Furthermore, the excellent correlation of IINS and MD results indicates that the interpretation of these results is reasonable and valid. However, cation charge density and framework charge are undoubtedly not the only variables which affect librational motions of nanoconfined water.

The general interpretation of the correlated IINS and power spectra suggests that both the cation charge density and the anionic field strength (i.e., Si/Al ratio) have significant impacts on the rotational motion of nanoconfined water. Furthermore, the balance between cation charge density and framework anionic field strength has a marked impact on the librational signatures of a given paired zeolite−ion system. The experimental data clearly illustrate that with the alteration of ion−water−zeolite equilibria conditions (which modify the librational signatures of nanoconfined water) a different localized environment results due to the cations within the zeolite pore. The results also indicate that electrostatic charge on the overall framework has a stronger influence than charge density of a given ion in the channel, and that these effects become more pronounced as the charge difference between ion and zeolite is increased. It is interesting to note that a shift to lower frequencies (in the power spectra) in the alkali metal series follows an inverse trend of increasing enthalpies of hydration for the given cation (ΔH_{hyd}: $Cs^+ < Rb^+ < K^+ < Na^+ < Li^+$; libration shift: $Cs^+ > Rb^+ > K^+ > Na^+ > Li^+$). This observation is reversed

in the alkaline earth metal series, with decreasing frequencies as a function of hydration enthalpy (ΔH_{hyd}: $Ba^{2+} < Sr^{2+} < Ca^{2+} < Mg^{2+}$; libration shift: $Ba^{2+} < Sr^{2+} < Ca^{2+} < Mg^{2+}$).

Similarities and difference in trends exist when comparing the zeolite experimental IINS data and MD derived power spectra. Comparison among the CLI series (Figures 2A, 2B, and 3) reveals a reversal in the libration shift trends between the monovalent and divalent series. In the observed IINS spectra, the CLI_{mono} series exhibits a decreasing trend with monovalent cations, while showing an increasing trend in librational edge frequency as a function of increasing ion charge densities. This behavior is also observed in the comparison of the IINS data for the HEU_{mono} and HEU_{di} series (Figures 2C, 2D, and 3). In our prior report,[12] the HEU power spectra exhibited the smallest magnitude frequency shift of all the zeolite−ion combinations studied. This response may indicate that the HEU system is near a critical point in the equilibrium between the ion−water and zeolite−water interactions where the energy of interaction changes from being dominated by the ion to being dominated by the zeolite.

Comparison of IINS spectra of CLI_{di} and HEU_{di} reveals a good agreement in trends between the two zeolite systems with frequency increasing as a function of increasing charge density ($Ca^{2+} < Mg^{2+}$). The data suggest that this behavior arises from a shift in ion−water−zeolite equilibria toward the stronger ion−water interactions over the diminished ion−zeolite or zeolite−water interactions. An additional contributing factor may be the more effective role of water−water and water−zeolite interactions in channels, especially in the divalent series where there are fewer counterbalancing extraframework cations than the more densely populated monovalent series.[39]

In some systems all three libration modes may not be observed, for example, if a particular mode is completely unhindered. Unfortunately, our MD simulations were not able to fully addresse this issue since there were multiple different, but closely related (energetically and structurally), "bulk-like" water configurations and as such precluded any direct assignment of discrete wagging, twisting, of rocking modes in the librational spectra. Density functional theory (DFT) studies and normal-mode analysis of small water clusters revealed that discrete librational modes are not distinguishable unless there are very few waters or the system is nearly static. None of the HEU or CLI systems we examined fit either of those criteria, and thus discrete assignments cannot be made with any degree of certainty. However, we suspect that all three librational modes are present and close in frequency in these systems and none are strongly suppressed due to interactions with the framework.

Conclusions

We have examined a subset of the alkali and alkaline earth metal series of cation analogues of clinoptilolite (Si/Al $\approx$ 5) and heulandite (Si/Al $\approx$ 3.5) frameworks using incoherent inelastic neutron scattering. Coupled with our prior MD studies, we have demonstrated that ion charge density and the electrostatic field of the zeolite (Si/Al ratios) have a strong impact on the dynamic intermolecular behavior of nanoconfined water. This impact is manifested and observable in librational region on the IINS spectra by shifting the data to higher frequencies. Furthermore, charge density of the framework (i.e., Si/Al ratios) has the greatest influence on librational motions, while the identity and charge of the extraframework cations is of less significance. Correlation of these data confirms the importance of ion−zeolite, ion−water, and water−zeolite equilibria on the rotational motions of water. The librational peaks in the IINS spectra for heulandite (the more negatively charged framework) are shifted to higher frequencies for the HEU_{mono} from the CLI_{mono}. The trend in the IINS spectra indicates that the increased electrostatic field associated with the zeolite channel produces more heavily restricted water molecule rotations (e.g., recognized by a shift to higher frequencies). This behavior becomes more pronounced as cation charge density increases. The HEU_{di} series exhibits the same general trend in the observed data, although this behavior occurs at a higher frequency. This behavior suggests that the higher cation field strength is further restricting the rotational motion of confined water. The notable reversal between experimental and simulated spectra for the HEU_{di} series is possibly due to a shift in equilibrium from being dominated by water−water to water−framework, although we do not fully understand this phenomenon yet.

The combined effect of these two variables provides a basic foundation to understanding the influence of exchangeable cation charge density and anionic field strength of the framework, and the effects that these opposing electrostatic fields have on the librational behavior. While the electrostatic field of the framework has the greatest effect, it is the overall differential between cation charge density and anion framework charge which is the core phenomenon that alters the librational dynamics of nanoconfined water. Furthermore, the balance between these fields is the foundational reason for ion exchange capacities and potential ion exchange rates. Future investigations could potentially include a combination of the thermodynamics of ion exchange and hydration processes, plus the structural analysis of hydrogen-bonded networks within these zeolite systems.

Acknowledgment. We would like to thank Louise J. Criscenti, Jeffery A. Greathouse, and James P. Larentzos for numerous helpful discussions and two anonymous referees for their valuable feedback. This work was supported in part by the Laboratory Directed Research and Development (LDRD) program of Sandia National Laboratories. Sandia National Laboratories is a multiprogram laboratory operated by Sandia Corporation, a Lockheed Martin Company, for the United States Department of Energy's National Nuclear Security Administration under Contract No. DE-AC04-94AL85000. This research is also sponsored by the United States Department of Energy under Contract No. W-7405-ENG-36. The work benefited from the use of the Manuel Lujan Jr. Neutron Scattering Center at Los Alamos National Laboratory, which is funded by the Department of Energy Office of Science, Basic Energy Sciences.

References and Notes

(1) Head-Gordon, T.; Hura, G. *Chem. Rev.* **2002**, *102*, 2651, and references therein.

(2) Kalinichev, A. G. In *Reviews in Mineralogy and Geochemistry*; Kubicki, J. D., Cygan, R. T., Eds.; 2001, Vol. 42, and references therein.

(3) Jedlovsky, P.; Brodholt, J. P.; Bruni, F.; Ricci, M. A.; Soper, A. K.; Vallauri, R. *J. Chem. Phys.* **1998**, *108*, 8528.

(4) Soper, K. *Chem. Phys.* **2000**, *258*, 121.

(5) Ricci, M. A.; Soper, A. K. *Physica A* **2002**, *304*, 43.

(6) Soper, A. K.; Ricci, M. A. *Phys. Rev. Lett.* **2000**, *84*, 2881.

(7) (a) Guillot, B. *J. Mol. Liq.* **2002**, *101*, 217. (b) Guillot, B. *J. Mol. Liq.* **2002**, *101*, 219.

(8) Head-Gordon, T.; Johnson, M. E. *Proc. Natl. Acad. Sci U.S.A.* **2006**, *103*, 7973.

(9) Wang, K.; Kalinichev, A. G.; Kirkpatrick, R. J. *Geochim. Cosmochim. Acta* **2004**, *16*, 3351.

(10) Ricci, M. A.; Bruni, F.; Gallo, P.; Rovere, M.; Soper, A. K. *J. Phys.: Condens. Matter* **2000**, *12*, 345.

(11) Ricci, M. A.; Rovere, M. *J. Phys. IV* **2000**, *10*, 187.

(12) Ockwig, N. W.; Cygan, R. T.; Nenoff, T. M.; Daemen, L. L.; Hartl, M. A.; Criscenti, L. J. *Phys. Chem. Chem. Phys.* **2008**, *10*, 800.

(13) Klafter, J.; Blumen, A.; Drake, J. M. In *Relaxation and Diffusion in Restricted Geometry*; Klafter, J., Drake, J. M., Eds.; Wiley: New York, 1989.

(14) Rupley, J. A.; Careri, G. *Adv. Protein Chem.* **1991**, *41*, 37.

(15) Arndt, M.; Stannarius, R.; Gorbatschow, W.; Kremer, F. *Phys. Rev. E: Stat., Nonlinear, Soft Matter* **1996**, *54*, 5377.

(16) *Proceedings of the First International Workshop of Dynamics in Confinement*; Frick, B., Zorn, R., Buttner, H., Eds; EDP Science: Les Ulis, France, 2000.

(17) (a) *J. Phys.: Condens. Matter* **2004**, *16*, Special Section on Water in Confined Geometries; Rovere, M., Guest Ed.; pp S5297−S5470. (b) Crupi, V.; Majolino, D.; Venuti, V. *J. Phys.: Condens. Matter.* **2004**, *16*, S5297. (c) Swenson, J. *J. Phys.: Condens. Matter* **2004**, *16*, S5317. (d) Puibasset, J.; Pellenq, R. J. M. *J. Phys.: Condens. Matter* **2004**, *16*, S5329. (e) Brovchenko, I.; Geiger, A.; Oleinikova, A. *J. Phys.: Condens. Matter* **2004**, *16*, S5345. (f) Zangi, R. *J. Phys.: Condens. Matter* **2004**, *16*, S5371. (g) Jedlovsky, P. *J. Phys.: Condens. Matter* **2004**, *16*, S5389. (h) Liu, L.; Faraone, A.; Mou, C. Y.; Yen, C. W.; Chen, S. H. *J. Phys.: Condens. Matter* **2004**, *16*, S5403. (i) Klein, J.; Raviv, U.; Perkin, S.; Kampf, N.; Chai, L.; Giasson, S. *J. Phys.: Condens. Matter* **2004**, *16*, S5437. (j) Webber, B.; Dore, J. *J. Phys.: Condens. Matter* **2004**, *16*, S5449.

(18) Angell, C. A. In *Water: A Comprehensive Treatise*; Franks, F., Ed.; Plenum Press: New York, 1981.

(19) Mizota, T.; Satake, N.; Fujiwara, K.; Nakayama, N. *Steam, Water, and Hydrothermal Systems: Physics, and Chemistry Meeting the Needs of Industry, Proceedings of the 13th ICPWS*; Tremaine, P. R., Hill, P. G., Irish, D. E., Balakrishnan, P. V., Eds.; NCR Research Press: Ottawa, ON, 2000.

(20) Beta, I. A.; Bohling, H.; Hunger, B. *Phys. Chem. Chem. Phys.* **2004**, *6*, 1975.

(21) Jobic, H.; Tuel, A.; Krossner, M.; Sauer, J. *J. Phys. Chem.* **1996**, *100*, 19545.

(22) Crupi, V.; Majolino, D.; Migliardo, P.; Venuti, V.; Wanderlingh, U.; Mizota, T.; Telling, M. *J. Phys. Chem. B* **2004**, *108*, 4314.

(23) Line, C. M. B.; Kearley, G. J. *J. Chem. Phys.* **2000**, *112*, 9058.

(24) Line, C. M. B.; Kearley, G. J. *Chem. Phys.* **1998**, *234*, 207.

(25) Celestian, A. J.; Parise, J. B.; Smith, R. I.; Toby, B. H.; Clearfield, A. *Inorg. Chem.* **2007**, *46*, 1081.

(26) Celestian, A. J.; Kubicki, J. D.; Hanson, J.; Clearfield, A.; Parise, J. B. *J. Am. Chem. Soc.* **2008**, currently under review.

(27) Soper, A. K. In *Hydrogen Bond Network*; Bellissent-Funel, M. C., Dore, J. C., Eds.; NATO ASI Series C: Mathematical and Physical Science; Kluwer Academic: Dordecht, 1994.

(28) Wiggins, P. M. *Prog. Polym. Sci.* **1988**, *13*, 1.

(29) Crupi, V.; Majolino, D.; Migliardo, P.; Venuti, V.; Wanderlingh, U.; Mizota, T.; Telling, M. *J. Phys. Chem. B* **2002**, *106*, 10884.

(30) Bellissent-Funel, M. C.; Dorbez-Sridi, R.; Bosio, L. *J. Chem. Phys.* **1996**, *104*, 1.

(31) Crupi, V.; Magazu, S.; Maisano, G.; Majolino, D.; Migliardo, P. *J. Mol. Liq.* **1999**, *80*, 133.

(32) Kaatze, U.; Uhlendorf, V. *Z. Phys. Chem. (N.F.)* **1981**, *126*, 151.

(33) Polnazek, C. F.; Bryant, R. G. *J. Chem. Phys.* **1984**, *81*, 4038.

(34) Gallo, P.; Ricci, M. A.; Rovere, M. *J. Chem. Phys.* **2002**, *116*, 342.

(35) Gallo, P.; Rapinesi, M.; Rovere, M. *J. Chem. Phys.* **2002**, *117*, 369.

(36) Murad, S.; Jia, W.; Krishnamurthy, M. *Mol. Phys.* **2004**, *102*, 2103.

(37) Demontis, P.; Stara, G.; Suffritti, G. B. *J. Chem. Phys.* **2004**, *120*, 9233.

(38) Shirono, K.; Endo, A.; Daiguji, H. *J. Phys. Chem. B* **2005**, *109*, 3446.

(39) Nenoff, T. M.; Ockwig, N. W.; Cygan, R. T.; Alam, T. M.; Leung, K.; Pless, J. D.; Xu, H.; Hartl, M. A.; Daemen, L. L. *J. Phys. Chem. C* **2007**, *111*, 13212.

(40) Fourzi, A.; Dorbez-Sridi, R.; Oumezzine, M. *J. Chem. Phys.* **2002**, *116*, 791.

(41) Crupi, V.; Majolino, D.; Migliardo, P.; Venuti, V.; Bellissent-Funel, M. C. *Mol. Phys.* **2003**, *101*, 3323.

(42) Kolesnikov, A. I.; Li, J. C. *Physica B* **1997**, *234*, 34, and references therein.

(43) Bellissent-Funel, M. C.; Lal, J.; Bosio, L. *J. Chem. Phys.* **1993**, *98*, 4246.

(44) Crupi, V.; Majolino, D.; Migliardo, P.; Venuti, V.; Diaonoux, A. J. *Appl. Phys. A: Mater. Sci. Process.* **2002**, *74*, S555.

(45) Venturini, F.; Gallo, P.; Ricci, M. A.; Bizzari, A. R.; Cannistraro, S. *J. Chem. Phys.* **2001**, *114*, 10010.

(46) (a) Anandan, S.; Okazaki, M. *Microporous Mesoporous Mater.* **2005**, *87*, 77. (b) Brühwiler, D.; Calzaferri, G. *Microporous Mesoporous Mater.* **2004**, *72*, 1. (c) Ma, Y.; Tong, W.; Zhou, H.; Suib, S. L. *Microporous Mesoporous Mater.* **2000**, *37*, 243.

(47) (a) Carey, J. W.; Bish, D. L. *Am. Mineral.* **1996**, *81*, 952. (b) Wilkin, R. T.; Barnes, H. L. *Phys. Chem. Miner.* **1999**, *26*, 468. (c) Yang, P.; Stolz, J.; Armbruster, T.; Gunter, M. E. *Am. Mineral.* **1997**, *82*, 517. (d) Doebelin, N.; Armbruster, T. *Microporous Mesoporous Mater.* **2003**, *61*, 85. (e) Ruiz-Salvador, A. R.; Gómez, A.; Lewis, D. W.; Catlow, C. R. A.; Rodriguez-Albelo, L. M.; Montero, L.; Rodriguez-Fuentes, G. *Phys. Chem. Chem. Phys.* **2000**, *2*, 1803. (f) Ruiz-Salvador, A. R.; Lewis, D. W.; Rubayo-Soneira, J.; Rodriguez-Fuentes, G.; Sierra, L. R.; Catlow, C. R. A. *J. Phys. Chem. B* **1998**, *102*, 8417. (g) Ruiz-Salvador, A. R.; Gómez, A.; Lewis, D. W.; Rodriguez-Fuentes, G.; Montero, L. *Phys. Chem. Chem. Phys.* **1999**, *1*, 1679.

(48) Zhao, D.; Szostak, R.; Kevan, K. *J. Mater. Chem.* **1998**, *8*, 233.

(49) Breck, D. W. In *Zeolite Molecular Sieves: Structure, Chemistry, and Use*; Wiley: New York, 1974.

(50) Elemental analysis performed by Galbraith Laboratories, Inc., Knoxsville, TN.

(51) Clinoptilolite series elemental analysis results. Na−CLI (calcd, %): Na, 5.10; Al, 5.99; Si, 31.17; H, 1.69. K−CLI (calcd, %): K, 8.25; Al, 5.70; Si, 30.24; H, 1.63. Rb−CLI (calcd, %): Rb, 15.78; Al, 4.98; Si, 28.01; H, 1.50. Mg−CLI (calc, %): Mg, 2.86; Al, 6.34; Si, 31.69; H, 1.73. Ca−CLI (calcd, %) Ca, 4.70; Al, 6.33; Si, 30.89; H, 1.70. Na−CLI (obsd, %): Na, 5.19; Al, 5.91; Si, 31.22; H, 1.81. K−CLI (obsd, %): K, 8.32; Al, 5.76; Si, 30.92; H, 1.78. Rb−CLI (obsd, %): Rb, 15.39; Al, 5.37; Si, 28.33; H, 1.71. Mg−CLI (obsd, %): Mg, 2.55; Al, 6.17; Si, 32.16; H, 2.01. Ca−CLI (obsd, %): Ca, 4.71; Al, 6.62; Si, 31.36; H, 1.29.

(52) Heulandite series elemental analysis results. Na−HEU (calcd, %): Na, 6.43; Al, 7.54; Si, 29.06; H, 1.67. K−HEU (calcd, %): K, 10.87; Al, 7.51; Si, 27.35; H, 1.59. Rb−HEU (calcd, %): Rb, 21.44; Al, 6.77; Si, 23.95; H, 1.40. Mg−HEU (calcd, %): Mg, 4.00; Al, 8.88; Si, 28.65; H, 1.71. Ca−HEU (calcd, %): Ca, 6.14; Al, 8.27; Si, 28.42; H, 1.67. Na−HEU (obsd, %): Na, 6.57; Al, 7.81; Si, 30.12; H, 2.00; Ca, 0.03; Fe, 0.01. K−HEU (obsd, %): K, 10.61; Al, 7.54; Si, 28.15; H, 1.98; Ca, 0.05; Fe, 0.02. Rb−HEU (obsd, %): Rb, 20.37; Al, 6.18; Si, 23.44; H, 2.13; Ca, 0.11; Fe, 0.07. Mg−HEU (obsd, %): Mg, 4.92; Al, 9.00; Si, 27.99; H, 1.83; Ca, 0.03; Fe, 0.03. Ca−HEU (obsd, %): Ca, 6.38; Al, 8.64; Si, 28.87; H, 1.99; Fe, 0.05.

(53) Clinoptilolite: $a = 17.66$ (7), $b = 17.92$ (5), $c = 7.40$ (1) Å, and $b = 116.43$ (14)°. Heulandite: $a = 17.62$ (24), $b = 17.92$ (21), $c = 7.46$ (13) Å, and $b = 116.34$ (53)°.

(54) (a) Debye, P. *Ann. Phys.* **1913**, *348*, 49. (b) Waller, I. *Z. Phys.* **1923**, *17*, 398. c.

(55) PeakFit v4.12 software suite with an error of ± 5 cm^{-1}.

(56) Li, J. C. *J. Chem. Phys.* **1996**, *105*, 6733.

(57) (a) Yildrim, T. *Chem. Phys.* **2000**, *261*, 205. (b) Payne, M. C.; Teter, M. P.; Arias, D. C.; Joannopoulos, J. D. *Rev. Mod. Phys.* **1992**, *64*, 1045. (c) Lovesey, S. In *Theory of Neutron Scattering in Condensed Matter*, 3rd ed.; Oxford University Press: New York, 1987.

(58) Li, J. C.; Ross, D. K. *Nature* **1993**, *365*, 327.

JP803770V